Alternative Cleavage of Alzheimer-Associated Presenilins During Apoptosis by a Caspase-3 Family Protease

Tae-Wan Kim, Warren H. Pettingell, Yong-Keun Jung, Dora M. Kovacs, Rudolph E. Tanzi*

Most cases of early-onset familial Alzheimer's disease (FAD) are caused by mutations in the genes encoding the presenilin 1 (PS1) and PS2 proteins, both of which undergo regulated endoproteolytic processing. During apoptosis, PS1 and PS2 were shown to be cleaved at sites distal to their normal cleavage sites by a caspase-3 family protease. In cells expressing PS2 containing the asparagine-141 FAD mutant, the ratio of alternative to normal PS2 cleavage fragments was increased relative to wild-type PS2-expressing cells, suggesting a potential role for apoptosis-associated cleavage of presenilins in the pathogenesis of Alzheimer's disease.

Apoptosis (programmed cell death) is an evolutionary conserved form of cellular suicide that plays a beneficial role during development and homeostasis (*1*). Extensive evidence indicates that activation of apoptotic cell death is associated with a variety of neurodegenerative disorders (*2*), including Alzheimer's disease (AD) (*3–5*). Most cases of early-onset FAD are caused by mutations in the genes encoding the PS1 and PS2 proteins (6), both of which undergo regulated endoproteolytic processing to yield two stable fragments (*7–9*). Overexpression of the presenilins in transfected cells has been reported to increase susceptibility to apoptosis (*10–12*). Here we investigated whether the presenilins serve as substrates for apoptosis-associated cleavage in the programmed cell death pathway and assessed the effects of an FAD mutation on this process.

We initially identified the endogenous form of the PS2 endoproteolytic COOH-terminal fragment (CTF) using the COOH-terminal antibody to PS2, anti-PS2Loop (*13*). The endogenous PS2-CTF appeared as a 25-kD band in both human brain (*14*) and in uninduced H4 neuroglioma cells (Fig. 1). As reported for PS1 (*7*), no full-length PS2 was detected in brain (*14*) or in the uninduced cells (Fig. 1). In stably transfected H4 cells that were induced to overexpress PS2 containing a COOH-terminal FLAG epitope tag (9), the 54-kD full-length and high molecular weight forms of PS2 were observed along with multiple CTFs with apparent sizes of 26, 25, and 20 kD (Fig. 1, lanes 1 and 8), representing the transgene-derived normal cleavage product containing the eight–amino acid FLAG epitope, the endogenous CTF, and a smaller, alternative CTF, respectively (*15*).

We have previously shown that overexpression of PS2 in transfected cells results in the generation of a 20-kD CTF that predominantly localizes to the detergent (Triton)-resistant cellular fraction and that exhibits a very slow rate of turnover (*9*, *15*). Whereas here the endogenous (Fig. 1, band e) and normal transgene-derived (Fig. 1, band f) CTFs were primarily localized to the detergent-soluble cellular fraction (Fig. 1, lane 3), the smaller, alternative 20-kD CTF was enriched in the detergent-resistant fraction (Fig. 1, lane 2). Together, these data suggested that when overexpressed in stably transfected inducible H4 cells, PS2 is cleaved at a site located distal to the normal cleavage site, resulting in a smaller detergent-insoluble CTF.

Given recent reports that overexpression of PS2 induces apoptosis in transfected cells (*10*, *12*), we examined the effects of zVAD, a broad-spectrum inhibitor for most mammalian interleukin-1β–converting enzyme ICE/Ced-3 proteases (caspases), and zDEVD-fmk, a more selective inhibitor for caspase-3 (CPP32) family proteases (caspases-3, -6, and -7) (*16*, *17*). Both zVAD and zDEVD blocked the generation of the 20-kD PS2-CTF in cells overexpressing PS2 (Fig. 1) but had no effect on levels of the endogenous 25-kD CTF (Fig. 1, band e), the 26-kD transgene-derived CTF (Fig. 1, band f), or other PS2 species. These findings indicated that in the absence of traditional apoptotic stimuli, overexpression of PS2 led to the activation of caspase-3 family proteases that alternatively cleaved PS2.

Caspase-3 is activated through a protease cascade in response to apoptotic stimuli and cleaves specific intracellular substrates during apoptosis (*16*, *17*). To determine whether the alternative PS2-CTF was generated from full-length PS2 during apoptosis, we used a relatively low-expressing inducible H4 cell line in which only low to undetectable levels of the 20-kD CTF were observed at 12 hours after induction of PS2. When apoptosis was induced with 20 μM etoposide, the alternative 20-kD CTF as well as the corresponding alternative NH_2-terminal fragment (NTF) were generated (Fig. 2). The alternative NTF was 34 kD, whereas the "normal" NTF, labeled as band f in the top panel of Fig. 2, was 30 kD. The alternative PS2 cleavage fragments were first observed at 3 hours after treatment with etoposide. Treatment with increasing concentrations of zVAD inhibited the generation of both alternative cleavage products (Fig. 2). These data indicated that full-length PS2 gave rise to the alternative NH_2- and COOH-terminal cleavage fragments after the induction of apoptosis.

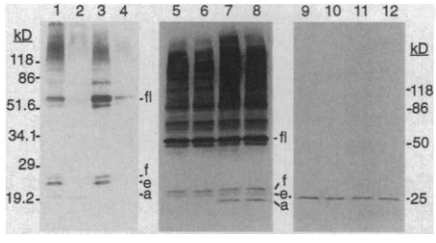

Fig. 1. Multiple PS2 COOH-terminal fragments (PS2-CTF) in the inducible H4 cells (*9*) overexpressing COOH-terminal epitope-tagged PS2. The 25-kD endogenous PS2 fragment (band e) was detected in both induced (lanes 1, 5 to 8) and uninduced (lanes 9 to 12) samples (*13*). Two additional fragments, including a 26-kD fragment representing the normal cleavage product containing an eight–amino acid FLAG epitope (band f), and the smaller, 20-kD fragment (band a), were detected only in the induced (lanes 1, 5 to 8) samples. The 20-kD CTF was selectively localized in the nonionic detergent (1% Triton X-100)–resistant cellular fraction (lane 2) (*9*, *13*). Wild-type PS2 cells were induced for 48 hours, fractionated into detergent-insoluble and -resistant (lane 2) and detergent-soluble (lane 3) fractions and wash (lane 4), and then analyzed by protein immunoblotting (*13*). Total SDS lysates are shown in lane 1. Generation of the 20-kD PS2-CTF was blocked by zVAD (zVAD-fmk, a broad-spectrum caspase inhibitor) and zDEVD (zDEVD-fmk, a selective caspase-3 inhibitor) in cells overexpressing PS2 (lanes 5, 6, 9, and 10). zFA (cathepsin B inhibitor) was used as a control for the fluoromethylketone (fmk) group (lanes 7 and 11). Inducible PS2 cells were incubated with 100 μM zVAD (lane 5 and 9), zDEVD (lanes 6 and 10), and zFA (lanes 7 and 11), or solvent alone (dimethylsulfoxide; lanes 8 and 12) in the absence (uninduced, lanes 9 to 12) or presence (induced, lanes 5 to 8) of tetracycline for 24 hours.

T.-W. Kim, W. H. Pettingell, D. M. Kovacs, R. E. Tanzi, Genetics and Aging Unit, Department of Neurology, Massachusetts General Hospital, Harvard Medical School, Charlestown, MA 02129, USA.
Y.-K. Jung, Department of Life Science, KwangJu Institute of Science and Technology, 572 Sangam-dong, Kwangsan-ku, KwangJu, Korea.

*To whom correspondence should be addressed. E-mail: tanzi@helix.mgh.harvard.edu

We next examined whether endogenous PS2 is also cleaved by a caspase-3 family protease (or proteases). When native H4 cells were treated with staurosporine (Fig. 3A) or etoposide (*14*), apoptosis was induced as indicated by poly(ADP-ribose) polymerase (PARP) cleavage, proteolysis of inactive caspase-3 precursor (CASP-3), and decreased viability (assayed by trypan blue exclusion) (*14*). The progression of apoptosis correlated with the increased generation of the endogenous 20-kD PS2-CTF and decreased production of the 25-kD CTF (starting at 6 hours after treatment) (Fig. 3A).

Alternative cleavage of endogenous PS2 during either staurosporine- or etoposide-induced apoptosis was specifically blocked by zVAD (Fig. 3B) and zDEVD (Fig 3C), both of which displayed no effect on normal processing of PS2 (generation of the 25-kD endogenous fragment). zVAD was a more potent inhibitor of apoptosis-induced cleavage of PS2 than zDEVD (*18*). This is most likely due to the fact that zVAD blocks the activation of the upstream protease cascade during the apoptotic pathway, whereas zDEVD specifically acts downstream as a competitive inhibitor for the caspase-3 cleavage site (*17*). These data indicated that in native H4 cells undergoing apoptosis, a caspase-3 family protease was responsible for the generation of the 20-kD PS2-CTF. Thus, like PARP (*19*) or lamins (*20*), PS2 appears to serve as an apoptotic death substrate that undergoes alternative proteolysis during apoptosis (*21*).

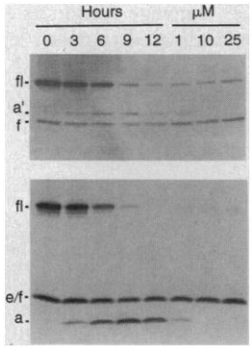

Fig. 2. Cleavage of full-length 54-kD PS2 (fl) by a zVAD-sensitive protease activated during etoposide-induced apoptosis. Inducible H4 cells expressing PS2 containing the NH_2-terminal FLAG epitope were induced for 12 hours and further incubated with media containing 20 μM etoposide for the time indicated, or first treated and incubated with the indicated concentrations of zVAD for 12 hours. Alternative (a′, 34 kD) and normal (f, 30 kD) NH_2-terminal cleavage products were detected by anti-FLAG (top) (*13*), and the alternative (a, 20 kD) and endogenous plus normal COOH-terminal cleavage products (e/f, 25 kD) were detected by anti-PS2Loop (bottom).

Differential cleavage by apoptotic and nonapoptotic proteases has also been demonstrated for the sterol-regulatory element binding proteins SREBP-1 and SREBP-2, endoplasmic reticulum proteins that control cellular cholesterol homeostasis (*22*). Both SREBP-1 and SREBP-2 are cleaved by caspase-3 (*23*) and caspase-3–related caspase-7 (*24*) at the site DSEPDSPVF for SREBP-1 and KDEPDSPPV for SREBP-2 (*25*). A potential consensus site (DSYDS, amino acids 326 to 330) (Fig. 4A) for cleavage by a caspase-3 family protease was localized in the large hydrophilic loop of PS2 (*26*). To test this site, we substituted either of the two Asp residues with Ala (Fig. 4A) (*27*). Both substitutions individually blocked the generation of the 20-kD CTF (Fig. 4B), indicating that PS2 is most likely cleaved after either Asp^{326} or Asp^{329}. The presence of Asp^{326} might also be required for cleavage after Asp^{329}, or vice versa. Meanwhile, the substitution $Asp^{308} \rightarrow Ala$ (D308A) had no effect on cleavage. These data demonstrate that a caspase-3 family protease most likely cleaves PS2 at the predicted consensus cleavage site (Asp-X) that resides distal to the normal cleavage site to yield the apoptosis-associated PS2-CTF.

To determine whether PS1 also undergoes alternative cleavage, we established inducible H4 cell lines expressing PS1 with a COOH-terminal FLAG epitope tag (*27*). In cells overexpressing high levels of PS1, in addition to the 24-kD "normal" transgene-derived CTF and the 23-kD endogenous CTF, a smaller, alternative 14-kD CTF was detected. However, in clonal cell lines expressing lower levels of PS1, the 14-kD CTF fragment was not detectable (*14*). As was observed for PS2, the generation of the alternative 14-kD PS1-CTF was blocked in the overexpressing cell lines by treatment with zVAD or zDEVD (*14*).

The 23-kD endogenous PS1-CTF was observed in native H4 cells as a doublet, presumably as a result of protein kinase C (PKC)–mediated phosphorylation of this fragment (*28*). Induction of apoptosis in native H4 cells with staurosporine led to

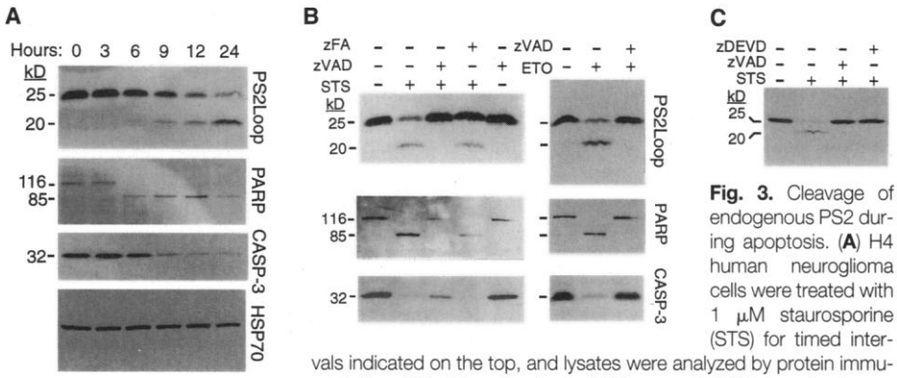

Fig. 3. Cleavage of endogenous PS2 during apoptosis. (**A**) H4 human neuroglioma cells were treated with 1 μM staurosporine (STS) for timed intervals indicated on the top, and lysates were analyzed by protein immunoblotting (*13*) with antibodies to PS2loop, poly(ADP-ribose) polymerase (PARP), pro-caspase-3 (CASP-3), and HSP70. (**B**) Inhibition of STS-induced (left) or etoposide (ETO)-induced (right) cleavage of PS2, PARP, and CASP-3 in H4 cells by zVAD. Cells were first treated with inhibitors for 1 hour, then further incubated in the presence or absence of 2 μM STS (left) or 20 μM etoposide (right) for 18 hours, and lysates were analyzed by protein immunoblotting (*13*). (**C**) Inhibition of apoptosis-induced cleavage of PS2 by zDEVD (inhibitor for a caspase-3 family protease; 100 μM). Treatment of cells with STS and inhibitors was similar to that described for (B).

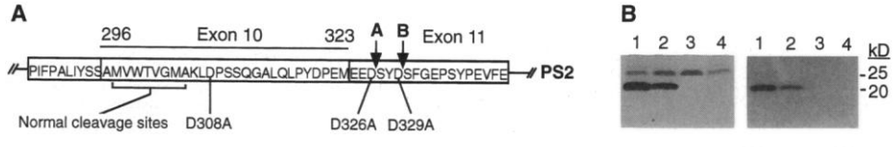

Fig. 4. Abolition of zVAD/zDEVD-sensitive cleavage of PS2 by replacement of Asp^{326} or Asp^{329}. (**A**) Consensus ICE/Ced-3 protease cleavage sites located after Asp^{326} or Asp^{329} (indicated by arrows A and B, respectively) at the PS2 loop domain encoded by exon 11. The predicted normal cleavage sites (*8*) are located in the distal region encoded by exon 10 (originally called exon 9) (*36*). Abbreviations for the amino acid residues are as follows: A, Ala; C, Cys; D, Asp; E, Glu; F, Phe; G, Gly; H, His; I, Ile; K, Lys; L, Leu; M, Met; N, Asn; P, Pro; Q, Gln; R, Arg; S, Ser; T, Thr; V, Val; W, Trp; and Y, Tyr. (**B**) Effect of D326A and D329A mutations on the generation of the 20-kD PS2 fragment (*27*). Inducible constructs encoding COOH-terminal FLAG epitope-tagged PS2 with indicated mutations (wild type, lane 1; D308A, lane 2; D326A, lane 3; and D329A, lane 4) were transiently transfected into tetracycline-responsive founder H4 cells (*9*). Cells were grown in the absence of tetracycline (induction) for 24 hours and further incubated in the presence of 20 μM etoposide for 9 hours and then analyzed by protein immunoblotting with either anti-PS2Loop (left) or anti-FLAG (right) (*13*).

the generation of the 14-kD PS1-CTF and also blocked the phosphorylation of the endogenous CTF (Fig. 5). This is consistent with the fact that staurosporine inhibits PKC activity. Etoposide-induced apoptosis also led to the generation of the 14-kD CTF but, as expected, did not block phosphorylation of the endogenous PS1-CTF (Fig. 5). As with PS2, apoptosis-associated cleavage of endogenous PS1 was blocked by the treatment with zVAD (Fig. 5) or zDEVD (*14*). The size of the alternative PS1-CTF and a scan of the PS1 amino acid sequence suggested that the consensus sequence AQRDS (amino acids 343 to 346) is the most likely site for caspase-3–related cleavage in PS1, although this will require direct testing.

To begin to investigate a potential role for apoptotic PS2 cleavage products in AD pathogenesis, we examined the effect of the Asn^{141}→Ile (N141I) Volga German FAD mutation (*29*) on the generation of the 20-kD PS2 CTF. Multiple wild-type or FAD mutant (N141I)-inducible cell lines expressing "low," "middle," or "high" amounts of PS2 were paired according to expression level and analyzed by protein immunoblotting (*13*). The ratio of the 20-kD CTF:26-kD CTF was increased approximately threefold in the PS2-N141I cells relative to the wild-type PS2 cells (Fig. 6) (*30*). Preliminary studies have also shown that the alternative 14-kD PS1-CTF accumulated in higher concentrations in lymphoblasts derived from patients with the Ala^{246}→Glu (A246E) PS1 FAD mutation as compared to those from age-matched controls (*31*).

Apoptotic cell death has been reported to be a pathological feature of AD (*3–5*), although the exact contribution of apoptosis to the pathogenesis of AD remains unclear. Our studies indicate that PS1 and PS2 participate in the apoptotic pathway. It is possible that the alternative endoproteolytic PS1 and PS2 fragments generated by a caspase-3 family protease (or proteases) under apoptotic conditions may serve as pro-apoptotic effectors that alter the apoptotic threshold, making cells more vulnerable to apoptosis. The observed increase in apoptotic PS2 fragments in cells overexpressing the FAD mutant PS2-N141I raises the possibility that this fragment may contribute to enhanced susceptibility to apoptosis as a result of this mutation (*10, 12*). The N141I FAD mutation in PS2 and other FAD defects in PS1 and PS2 lead to increased production of amyloid-β42 (Aβ42) in fibroblasts and plasma of FAD patients as well as in transfected cells and transgenic mice expressing mutant PS genes (*32*). In addition, treatment of cells with Aβ induced apoptotic neuronal death in vitro (concentrations of 1 to 100 μM) and in vivo (*3–5, 33*) and down-regulated anti-apoptotic Bcl-2 expression in primary neurons (concentration of 100 nM) (*34*). Collectively, these observations suggest at least two potential pathogenic pathways: (i) alternative PS cleavage products directly participate in inducing pro-apoptotic conditions, which in turn lead to pathogenic changes associated with FAD, including neuronal and synaptic degeneration and subsequent generation of Aβ42; and (ii) alternative PS cleavage products induce the increased production or accumulation of Aβ42 that, in turn, effects pro-apoptotic changes and neuronal cell death.

Because the alternative cleavage of the presenilins occurs within 3 hours after an apoptotic stimulus (Fig. 2), our findings suggest that the alternative clip most likely precedes the effects of PS2-N141I on the processing of amyloid precursor protein, leading to an increased ratio of Aβ42:Aβ40 in transfected cells (*32*). The PS2-N141I mutation increases both the ratio of Aβ42:Aβ40 (*32*) and the ratio of the alternative:normal PS2 COOH-terminal fragments by roughly three- to fourfold. Thus, these molecular events may be intimately related consequences of the PS2-N141I mutation. Exactly how the activation of caspase-3, the enhanced generation of alternative presenilin cleavage fragments, and the increased generation of Aβ42 interact to contribute to AD neuropathogenesis will be an important topic for future studies.

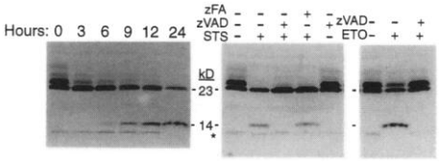

Fig. 5. Cleavage of endogenous PS1-CTF during STS-induced apoptosis. Samples identical to those used for Fig. 3 were stained with anti-PS1Loop (*7*). PS1 was cleaved to generate the smaller 14-kD fragment during the progression of apoptosis (left). Inhibition of STS-induced (middle) and etoposide-induced (right) PS1 cleavage by zVAD is shown. Asterisk indicates nonspecific bands.

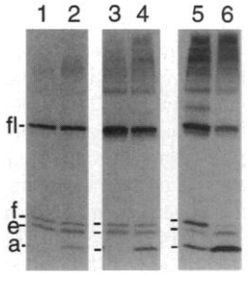

Fig. 6. Relative increase of the 20-kD PS2 CTF in H4 cells expressing N141I mutant (Volga German) PS2. The CTFs generated from inducible H4 cells expressing "low" (lanes 1 and 2), "middle" (lanes 3 and 4), and "high" (lanes 5 and 6) levels of wild-type (lanes 1, 3, and 5) and N141I FAD mutant (lanes 2, 4, and 6) PS2 (with COOH-terminal FLAG epitope tag) were detected by protein immunoblotting with anti-PS2Loop (*13*). In each case, the wild-type and PS2-N141I clonal cell lines were paired for similar levels of expression (*30*).

REFERENCES AND NOTES

1. M. D. Jacobson, M. Weil, M. C. Raff, *Cell* **88**, 347 (1997).
2. C. B. Thompson, *Science* **267**, 1456 (1995).
3. E. M. Johnson, *Neurobiol. Aging* **15**, 5187 (1994).
4. C. W. Cotman and A. J. Anderson, *Mol. Neurobiol.* **10**, 19 (1995).
5. A. LeBlanc, *Molecular Mechanism of Dementia* (Humana, Totowa, NJ, 1996), pp 57–71.
6. R. E. Tanzi *et al.*, *Neurobiol. Dis.* **3**, 159 (1996); J. Hardy, *Trends Neurosci.* **20**, 154 (1997).
7. G. Thinakaran *et al.*, *Neuron* **17**, 181 (1996).
8. M. B. Podlisny *et al.*, *Neurobiol. Dis.* **3**, 325 (1997).
9. T.-W. Kim *et al.*, *J. Biol. Chem.* **272**, 11006 (1997).
10. B. Wolozin *et al.*, *Science* **274**, 1710 (1996).
11. Q. Guo *et al.*, *Neuroreport* **8**, 379 (1996).
12. G. Deng, C. J. Pike, C. W. Cotman, *FEBS Lett.* **397**, 50 (1996).
13. The anti-PS2Loop is a PS2-specific antibody raised against the large hydrophilic loop domain following predicted transmembrane domain six of PS2 (*7*). Protein quantitation, SDS–polyacrylamide gel electrophoresis (PAGE; 4 to 20% or 16%), and protein immunoblotting were done as described (*9*) except that the lysis buffer [10 mM tris-HCl (pH 7.4), 150 mM NaCl, 1% Triton X-100, 0.5% NP-40, 5 mM EDTA plus either 0.3% SDS or 1% Sarkosyl] contained protease inhibitors, allowing for the efficient extraction of the 20-kD COOH-terminal fragment from the detergent-resistant fractions. Except in Figs. 1B and 3C (4 to 20% gradient gel), all SDS-PAGE was performed with 16% gels.
14. T.-W. Kim and R. E. Tanzi, unpublished data.
15. The 26- and 20-kD CTFs were absent in the uninduced samples (Fig. 1, lanes 9 to 12) and could be immunoprecipitated with antibodies to the FLAG epitope (*14*), indicating that these fragments were derived from the PS2 transgene. The 26-kD fragment is most likely the normal 25-kD cleavage product plus the eight–amino acid FLAG epitope tag. In the previous study (*9*), the regulated 26-kD normal cleavage product was not detectable on protein immunoblots with the relatively insensitive antibody to FLAG. As shown for PS1 (*7*), the generation of the normal PS2-CTF appears to be a regulated endoproteolytic event. This is evidenced by the observation that levels of the 26-kD transgene-derived PS2-CTF were not considerably greater than those of the native 25-kD CTF in the uninduced cells. Additionally, levels of the native 25-kD CTF were diminished in the induced cells, suggesting that the production of the transgene-derived CTF led to an attenuation in the amount of endogenous CTF. A similar type of "replacement" phenomenon has been reported for PS1 in transgenic mice expressing human PS1 (*7*). In contrast, the alternative 20-kD PS2-CTF did not appear to be generated in a regulated fashion (*9*).
16. E. S. Alnemri *et al.*, *Cell* **87**, 171 (1996).
17. S. J. Martin and D. R. Green, *ibid.* **82**, 349 (1995); A. M. Chinnaiyan and V. M. Dixit, *Curr. Biol.* **6**, 555 (1996).
18. Relative amounts of 20-kD PS2 fragments from the cells cotreated with 1 μM STS (18 hours) plus either zVAD or zDEVD (1 to 200 μM) were measured by transmittance analysis of the protein immunoblot as described (*13, 35*). Twenty-five micromolar zVAD was as effective as 100 μM zDEVD in inhibiting apoptosis-induced cleavage of PS2. The amounts of 20-kD fragments from the cells treated with STS alone were standardized as 100%.
19. S. H. Kaufman *et al.*, *Cancer Res.* **53**, 3976 (1993).

20. Y. A. Lazebnik *et al.*, *Proc. Natl. Acad. Sci. U.S.A.* **92**, 9042 (1995); N. Neamati *et al.*, *J. Immunol.* **154**, 1693 (1994).
21. In addition to H4 human neuroglioma cells, all findings were confirmed in native SK-N-SC neuroblastoma cells (*14*).
22. M. S. Brown and J. L. Goldstein, *Cell* **89**, 331 (1997).
23. X. Wang *et al.*, *EMBO J.* **15**, 1012 (1996).
24. J.-T. Pai, M. S. Brown, J. L. Goldstein, *Proc. Natl. Acad. Sci. U.S.A.* **93**, 5437 (1996).
25. X. Wang *et al.*, *J. Biol. Chem.* **270**, 18044 (1995).
26. Alternative endoproteolysis sites for PS2 are localized within the domain after predicted transmembrane domain 5, encoded by exon 11 (formerly exon 10) (*36*).
27. The point mutations in the potential aspartate cleavage sites of PS2 (D326A and D329A) and control aspartate (D308A) were introduced into a PS2 open reading frame by site-directed mutagenesis with Muta-Gene phagemid kit (Bio-Rad). The inducible construct encoding the full-length PS1 with 3′ FLAG epitope sequence was generated as described for PS2 (*9*). To establish the inducible PS1 cells, we sequenced the resulting constructs and stably transfected them into the H4 human neuroglioma founder cell line as described for the PS2-inducible cells (*9*).
28. M. Seeger *et al.*, *Proc. Natl. Acad. Sci. U.S.A.* **94**, 5090 (1997); J. Walter *et al.*, *ibid.*, p. 5349.
29. E. Levy-Lahad *et al.*, *Science* **269**, 973 (1995).
30. Values (mean ± SD, $n = 30$; $^*P < 0.05$) representing the ratios of alternative:normal CTF in multiple wild-type and FAD mutant (N141I) PS2 clonal lines induced for 24 hours were determined (*13*, *36*). Data from three independent experiments with five different wild-type and mutant PS2 clonal lines paired according to expression level were used.
31. D. M. Kovacs, T.-W. Kim, R. E. Tanzi, unpublished data.
32. D. Scheuner *et al.*, *Nature Med.* **2**, 864 (1996); T. Tomita *et al.*, *Proc. Natl. Acad. Sci. U.S.A.* **94**, 2025 (1997); D. R. Borchelt *et al.*, *Neuron* **17**, 1005 (1996); M. Citron *et al.*, *Nature Med.* **3**, 67 (1997); K. Duff *et al.*, *Nature* **383**, 710 (1996); W. Xia *et al.*, *J Biol. Chem.* **272**, 7977 (1997).
33. G. Forloni *et al.*, *Neuroreport* **4**, 523 (1993); D. Loo *et al.*, *Proc. Natl. Acad. Sci. U.S.A.* **90**, 7951 (1993); F. M. LaFerla *et al.*, *Nature Genet.* **9**, 21 (1995).
34. E. Paradis *et al.*, *J. Neurosci.* **16**, 7533 (1996).
35. A. I. Bush *et al.*, *Ann. Neurol.* **32**, 57 (1992).
36. J. Perez-Tur *et al.*, *Neuroreport* **7**, 297 (1995).
37. We thank G. Thinakaran and S. Sisodia for antibodies and J. Henderson for technical assistance. Supported by grants from the National Institute on Aging, National Institute of Neurological Disorders and Stroke, and the Metropolitan Life Foundation. R.E.T. is a Pew Scholar, D.M.K. is a French Foundation Fellow, and T.-W. K. is a recipient of a National Research Service Award.

14 May 1997; accepted 17 June 1997

Differential Effects of Early Hippocampal Pathology on Episodic and Semantic Memory

F. Vargha-Khadem,* D. G. Gadian, K. E. Watkins, A. Connelly, W. Van Paesschen, M. Mishkin

Global anterograde amnesia is described in three patients with brain injuries that occurred in one case at birth, in another by age 4, and in the third at age 9. Magnetic resonance techniques revealed bilateral hippocampal pathology in all three cases. Remarkably, despite their pronounced amnesia for the episodes of everyday life, all three patients attended mainstream schools and attained levels of speech and language competence, literacy, and factual knowledge that are within the low average to average range. The findings provide support for the view that the episodic and semantic components of cognitive memory are partly dissociable, with only the episodic component being fully dependent on the hippocampus.

One influential view of memory organization (*1*) pictures the cognitive or declarative form, comprising both fact and event memory, as a unitary process that is dependent on the hippocampal system, a set of heavily interconnected medial temporal-lobe structures consisting of the hippocampus and underlying entorhinal, perirhinal, and parahippocampal cortices. According to this notion, both fact (or semantic) memory and event (or episodic) memory are impaired together in a graded manner depending on the extent of damage to the hippocampal system as a whole. An earlier view (*2*), which still has its adherents (*3*), proposed instead that the core defect in temporal-lobe amnesia is a loss of context-rich episodic memory, in that in some amnesic cases, semantic memory, which is free of context, appears to have been relatively preserved. An opportunity to assess these different views has been provided by our study of patients with amnesia due to hippocampal pathology sustained, in two of our patients, very early in life, before they had acquired the knowledge base that characterizes semantic memory. The results suggest a possible reconciliation of the two views, namely that episodic memory depends primarily on the hippocampal component of the larger system, whereas semantic memory depends primarily on the underlying cortices.

Previously, in the absence of any reported cases of amnesia due to very early bilateral injury to the medial temporal lobe (*4*), it had seemed that such early damage might so impede cognitive development that the resulting syndrome would take the form, not of amnesia, but of severe mental retardation (*5*). The findings described here show instead that early bilateral pathology that is limited largely to the hippocampus produces a severe loss of episodic memory but leaves general cognitive development, based mainly on semantic memory functions, relatively intact.

The first of our three patients (*6*), Beth, now aged 14, was born after a difficult delivery, and she remained without a heartbeat for 7 to 8 min before being resuscitated. She also sustained injury to the right brachial plexus. Two hours after resuscitation, she had a generalized seizure, and such attacks recurred sporadically for 2 to 3 days despite treatment with anticonvulsant medication. Within 2 weeks, however, Beth had made a good recovery, although the brachial plexus injury resulted in permanent impairment of the right arm and hand due to partial loss of the nerve function deriving from the fifth and sixth cervical nerve roots. No other neurological problems were evident until she reached age 5 when memory difficulties were first noted on her entrance into a mainstream school. The second patient, Jon, now aged 19, was delivered prematurely at 26 weeks of gestation. Weighing just under 1 kg and suffering from breathing problems, he was kept in an incubator for 2 months, during which time he was tube-fed and placed on a ventilator. Thereafter, he improved steadily and developed normally. At the age of 4, he suffered two, protracted (1.5 to 2 hours), afebrile convulsions. His memory impairment was first noted by his parents about a year and a half after the two long-lasting attacks. The third patient, Kate, now aged 22, was an average student until the age of 9, when she accidentally received a toxic dose (400 mg for 3 days) of theophylline, a drug with which she was being treated for asthma. An acute episode of seizures, unconsciousness, and respiratory arrest ensued, from which she showed good physical recovery but which left her profoundly amnesic. Subsequently, at age 17, she developed temporal lobe epilepsy, which has been well controlled with anticonvulsant medication.

Neuropsychological examination showed

F. Vargha-Khadem and K. E. Watkins, Cognitive Neuroscience Unit, Institute of Child Health, University College London Medical School, Wolfson Centre, Mecklenburgh Square, London WC1N 2AP, UK.
D. G. Gadian and A. Connelly, Radiology and Physics Unit, Institute of Child Health, University College London Medical School, 30 Guilford Street, London WC1N 1EH, UK.
W. Van Paesschen, Radiology and Physics Unit, Institute of Child Health, University College London Medical School, 30 Guilford Street, London WC1N 1EH, UK, and Institute of Neurology, Queen Square, London WC1N 3BG, UK.
M. Mishkin, Laboratory of Neuropsychology, National Institutes of Mental Health, 49 Convent Drive, Bethesda, MD 20892–4415, USA.

*To whom correspondence should be addressed. E-mail: fkhadem@ich.ucl.ac.uk